

pubs.acs.org/JPCB Article

Rational Modulation of pH-Triggered Macromolecular Poration by Peptide Acylation and Dimerization

Published as part of The Journal of Physical Chemistry virtual special issue "Computational and Experimental Advances in Biomembranes".

Eric Wu, Ramsey M. Jenschke, Kalina Hristova, and William C. Wimley*



Cite This: J. Phys. Chem. B 2020, 124, 8835-8843



Read Online

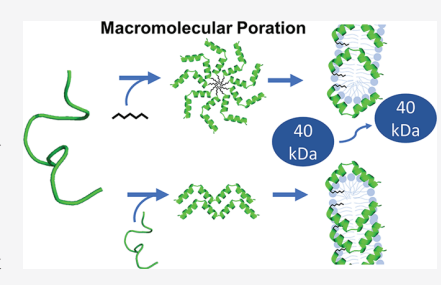
ACCESS

Metrics & More

Article Recommendations

Supporting Information

ABSTRACT: The synthetically evolved pH-dependent delivery (pHD) peptides are a unique family that bind to membranes, fold into α -helices, and form macromolecule-sized pores at low concentration at pH < 6. These peptides have potential applications in drug delivery and tumor targeting. Here, we show how pHD peptide activity can be modulated without changing the amino acid sequence. We increased the hydrophobicity of a representative peptide, pHD108 (GIGEVLHELAEGLPELQEWIHAAQQLGC-amide), by coupling hydrophobic acyl groups of 6–16 carbons and by forming dimers. Unlike the parent peptide, almost all variants showed activity at pH 7. This was due to strong partitioning into phosphatidylcholine vesicle bilayers and induced helix formation. The dimer maintained some pH sensitivity while being the most active



peptide studied in this work, with macromolecular poration occurring at 1:2000 peptide:lipid at pH 5. These results confirm that membrane binding, rather than pH, is the determining factor in activity, while also showing that acylation and dimerization are viable methods to modulate pHD108 activity. We propose a possible toroidal pore architecture with peptides in a parallel or mixed parallel/antiparallel orientation without strong electrostatic interactions between peptides in the pore as evidenced by a lack of dependence of activity on either pH or salt concentration.

INTRODUCTION

The design of pH-triggered, membrane-active peptides is inspired by applications such as tumor targeting and drug or nucleic acid delivery into cells. 1-5 In the pioneering work done by Subbarao et al., the pH-triggered influenza hemagglutinin fusion protein was used as a template to design a synthetic membrane permeabilizing peptide with pH-dependent activity. Szoka and colleagues later showed that the de novo designed peptide GALA-induced pH-triggered permeabilization of lipid vesicles to small molecules. In lipid vesicles, GALA does not release macromolecules, but it has been reported to increase the endosomal escape of nucleic acids for increased transfection efficiency.^{9,10} The peptide pHLIP, which is based on a transmembrane helix from the membrane protein bacteriorhodopsin, inserts across membranes as a monomer by translocating its C-terminus in a pH-dependent manner. 11 This peptide is undergoing clinical trials as an imaging agent in breast cancer because the peptide inserts into cancer cells due to the acidic microenvironment found in tumors. 12-15 The pHtriggered properties of GALA and PHLIP are based on the premise that protonatable aspartate and glutamate residues with helical *i* to i + 3 and *i* to i + 4 spacings inhibit the active α -helical secondary structure from forming at neutral pH due to electrostatic repulsions. Thermodynamic coupling between binding, folding, and protonation shifts the pK_a of at least

some of these acidic groups toward neutral, giving rise to pH-triggered activity in the useful range of 5–7. While these basic principles are well-understood, ¹⁶ most pH-triggered membrane permeabilizing peptides do not have both high potency and the ability to form large macromolecule-sized pores, two properties that would be very beneficial in applications using pH-triggered membrane-active peptides.

We have identified peptides with these two desirable properties through two generations of synthetic molecular evolution. First, Krauson et al. performed synthetic molecular evolution using a peptide library based on the helical cytolytic bee venom peptide melittin. This screen enabled the identification of the gain-of-function melittin analogue MelP5, which is much more potent than melittin and forms macromolecule-sized pores in phosphatidylcholine bilayers at low concentration. The parent sequence melittin permeabilizes membranes to small molecules by a mechanism that does not involve the formation of explicit membrane-spanning pores

Received: June 13, 2020 Revised: September 5, 2020 Published: September 7, 2020





under most conditions. 18,19 Next, Wiedman et al. used MelP5 as a template to design a library containing acidic aspartate and glutamate residues with helical spacings, enabling selection for pH-dependent membrane activity. The screen led to the identification of the pHD peptide family. At pH ≥ 7 , the pHD peptides are inactive, but at pH ≤ 6 they form very large macromolecule-sized pores in phosphatidylcholine bilayers. This unique activity occurs at peptide to lipid ratios (P:L) as low as $1:1000.^{20}$

The unique activity of the pHD peptides was recently studied by Kim et al., who showed that they induce large pores that are stable or metastable and have pore radii of up to \sim 8 nm in 1-palmitoyl-2-oleoyl-sn-glycero-3-phosphocholine (POPC) bilayers. Interestingly, the governing factor for the poration activity was the concentration of peptide bound to the bilayers. Once the effect of pH on binding was accounted for, no additional effects of pH were observed on secondary structure, pore structure, or activity across a wide range of acidic pH values. Leakage of 50% of a 40 kDa dextran from phosphatidylcholine vesicles occurred when \sim 75 peptides were bound to each 0.1 μ m diameter unilamellar vesicle at all pH values where leakage could be tested, between pH 4.5 and 6.5. This very high potency is shared only with the pH-insensitive macrolittins which were selected by us from the same library in a related screen. 21,22

Macromolecular poration at low peptide concentration is a highly unusual activity that must require a specific pore architecture. We currently have only the most basic information about the pore structure. We have shown that the pores are formed by peptides with a membrane-spanning orientation, ^{17,22} and we have speculated that these amphipathic peptides stabilize the boundary between the lipid bilayer and the water filled pores. ²² However, we do not know whether the pore is toroidal in nature, in which case peptides interact mainly with lipids, ²³ or has a barrel-stave architecture in which there are specific lateral interactions between peptides. The lack of information about the pore also means that we do not know how to best modulate the activity of the pHD peptides.

Here, we explore how macromolecular poration can be rationally modulated. We test the hypothesis that the activity and pH-dependence of this family of peptides can be altered by increasing membrane binding. We increased pHD peptide hydrophobicity, without changing the amino acid sequence, through acylation of the peptide termini and by dimerization of the peptide through C-terminal disulfide bond formation. We reasoned that such modifications could increase potency or shift the pH dependence by increasing partitioning into membranes.²¹ We further reasoned that pHD peptide modifications will only support macromolecular poration if they are compatible with the pore structure. Long terminal acyl chains, for example, could insert into the bilayer parallel to the lipid chains, thus potentially inhibiting activity if that orientation is inconsistent with the structure required for macromolecular poration. However, we find here that acylated peptides are highly active, showing that the pore structure is compatible with having either peptide terminus tethered to the bilayer interface. Likewise, dimers are highly active, showing that macromolecular poration is compatible with having at least some peptides in the pore with roughly parallel orientations and with their C-termini relatively close together. Thus, by testing the effects of these modifications, our experiments revealed constraints on the possible structure of the pore.

To explore the pore structure further, we reasoned that if a tightly packed barrel-stave pore is required for macromolecular

poration, the lateral interactions between peptides must include either favorable or unfavorable electrostatic interactions because pHD108 is highly charged, with eight ionizable groups, five acidic and three basic groups. To test the hypothesis of a barrel-stave pore, we compared macromolecular poration in situations where the peptide is fully bound at both pH 5 and pH 7, and we also measured macromolecular poration at very low and very high salt concentrations. We find little to no effect of pH or salt, a result that is consistent with a toroidal or disordered toroidal pore²⁴ rather than a tightly packed barrel-stave pore.

■ MATERIALS AND METHODS

Materials. Peptides were custom ordered from BioSynthesis, Inc., with an amide modification at the C-terminus. 1-Hexanethiol, 1-dodecanethiol, 1-hexadecanethiol, thiocholesterol, and dodecanoic anhydride were purchased from Millipore Sigma. 8-Aminonaphthalene-1,3,6-trisulfonic acid disodium salt (ANTS) and p-xylene-bis-pyridinium bromide (DPX) were purchased from Thermo Fisher Scientific. POPC was purchased from Avanti Polar Lipids, Inc. TAMRA-biotin-dextran (40 kDa) was synthesized and purified as described elsewhere. 8

Acylation and Dimerization of pHD108. pHD108, modified by the addition of a GC dipeptide at the C-terminus, was used for disulfide conjugation. For pHD108-C6, -C12, and -C16, the reaction mixture consisted of 250 μ M pHD108-GC, 12.5~mM thiol-lipid, and 0.1% DIPEA all in 10% water, 40%DMSO, and 50% methanol; this was incubated overnight at 57 °C and then purified by RP-HPLC (Shimadzu) with a Nucleodur C2 column (Macherey-Nagel) in an oven at 65 °C, with acetonitrile and water HPLC solvents (with 0.1% trifluoroacetic acid). Molecular weights of purified products were verified by MALDI-TOF mass spectrometry. N-terminus conjugation was performed with 200 µM pHD108, 10 mM dodecanoic anhydride, 2% DIPEA, and 70% DMF; this was incubated for 1 h at 23 °C, and then purified and verified as above. HPLC purified variants were lyophilized and then dissolved in DMSO; these were then run on HPLC to confirm purity (Figure S1).

Vesicle Leakage Assays. POPC large unilamellar vesicles (LUV) (0.1 μ m diameter) were prepared by suspending 50 μ mol of POPC in 1 mL of pH 5 or pH 7 buffer with either 12.5 mM ANTS and 45 mM DPX or 1 mg/mL TAMRA and biotin labeled 40 kDa dextran (TBD). The buffer used was 10 mM sodium phosphate (pH 7) or 10 mM sodium acetate (pH 5), both with 100 mM KCl. TBD leakage at high and low salt concentration was done similarly but with vesicles and buffer containing either 0 mM or 500 mM KCl. The LUVs were subjected to 10 freeze-thaw cycles and were then extruded 10 times through a 0.1 μ m polycarbonate membrane using a gas extruder. ANTS/DPX vesicles were separated from free ANTS and DPX using a G-100 Sephadex gel filtration column. Nonencapsulated TBD was removed with high-capacity streptavidin agarose beads (Thermo Fisher). Lipid concentration was determined with a modified Stewart assay.²⁵

Vesicle Binding and Trp Fluorescence. Binding was determined by recording Trp fluorescence of the conjugates in the presence of increasing concentrations of POPC vesicles. A solution of $10~\mu\mathrm{M}$ conjugate was prepared in pH 5 or 7 buffer in a quartz cuvette. POPC LUVs were added incrementally up to 3 mM. The volume increase due to each addition was $\leq 2~\mu\mathrm{L}$ into $150~\mu\mathrm{L}$ and was therefore negligible. Fluorescence spectra $(300-400~\mathrm{nm})$ were recorded in the absence of POPC and again 45 min after each addition of POPC LUV. The

fluorometer used was made by Horiba, with excitation fixed at 295 nm. Correction of fluorescence due to POPC scattering was performed as described in the study from Ladokhin et al. 26 The correction was determined by titrating concentrated POPC into a solution of 10 $\mu\rm M$ tryptophan and collecting the spectra for each titration. The difference of values at the critical wavelength of 337 nm, where intensity measurements were made for binding curves, was less than 10% at 1 mM and below, the concentration range at which $K_{\rm X}$ is determined. The intensity of the variants was measured as described above, and the intensity values at 337 nm were multiplied by the correction factor for the appropriate POPC concentration.

Mole fraction partition coefficient was calculated as

$$I/I_0 = 1 + \Delta I K_x L / (K_x L + W) \tag{1}$$

where I is the fluorescence intensity at 337 nm, I_0 is the intensity in buffer, ΔI is the increase in intensity due to peptide binding, K_x is the mole fraction partition coefficient, L is the concentration of lipid, and W is the concentration of water, 55.3 M.

Binding kinetics were modeled as a single exponential association

$$(I - I_0)/\Delta I = 1 - (\exp^{-kt})$$
 (2)

where ΔI is the increase in intensity over I_0 , the initial intensity. Because some binding rates were fast, we estimated k from $t_{0.9}$ by $k = -(\ln(0.1)/t_{0.9})$. The half-time, $t_{1/2}$, is $-(k/\ln(0.5))$.

Circular Dichroism (CD). pH 5 and pH 7 POPC vesicles were prepared as above but without KCl. Samples were also prepared in buffer without KCl and at 30 μ M peptide and \pm 0.5 mM POPC vesicles. CD was collected using a Jasco J-810 spectrapolarimeter, flushed with N₂. Scans were at 20 nm/s, 3 accumulations, and samples were at room temperature. The quartz cuvette path length was 0.1 cm. The spectra for a given sample was calculated by first subtracting the no peptide sample (blank) values and then zeroing the spectra to the average θ value from 250 to 260 nm. The mean residue ellipticity (MRE) was then calculated by the equation

$$MRE = \varepsilon/(Cn) \tag{3}$$

where ε is the ellipticity, C is the molar concentration of peptide, and n is number of residues.

RESULTS

Membrane Binding. To increase the hydrophobicity of pHD108 without changing its amino acid sequence, we conjugated a set of acyl chains to the termini of pHD108. Linear thioacyl groups of 6, 12, and 16 carbons were coupled to a C-terminal cysteine residue via a disulfide linkage (Figure 1). To compare the effects of C-terminal and N-terminal lipidation, we also coupled a linear C12 chain to the amino terminus by an amide bond. The added groups cover a broad range of hydrophobicity. The C6, C12, and C16 chains have log P values of 3.1, 6.1, and 8.1, respectively (Figure S1). We also generated the disulfide cross-linked dimer of pHD108, which has an increased hydrophobicity without acylation. To keep comparisons consistent, concentrations listed herein for the dimer are expressed relative to pHD108 monomer. We also coupled a thiocholesterol to the C-terminus of pHD108 and purified the conjugate, but it had such a low aqueous solubility that it could not be used in any of the experiments described below.

Conjugate	Abbrev.	Structure
pHD108		200,000
pHD108-C6	P-C6	S-S-
pHD108-C12	P-C12	56 M S-S
pHD108-C16	P-C16	
C12-pHD108	C12-P	NH-
pHD108 dimer	P-dimer	John S. S. Contraction

Figure 1. PHD108 conjugates synthesized and tested in this work. The peptide pHD108 was synthesized with a -GC dipeptide added to the C-terminus (GIGEVLHELAEGLPELQEWIHAAQQLGC-amide). Linear thioacyl groups of 6, 12, and 16 carbons were conjugated to the C-terminus using disulfide bonds. A linear C12 fatty acid was coupled to the N-terminus through an amide bond of a peptide lacking the GC dipeptide. A peptide dimer was formed by disulfide bond oxidation. The α -helical structure of pHD108, which is interrupted by the helix breaking proline residue at position 14, is shown schematically.

To determine how acylation and dimerization affect binding to membranes, we measured the fluorescence of the single tryptophan in the peptide after equilibration with increasing concentrations of lipid vesicles made of 1-palmitoyl-2-oleoyl-snglycero-3-phosphocholine (POPC), a widely used generic mimic of eukaryotic membranes. The change in fluorescence with lipid concentration (Figure 2A-C) enables determination of the partition coefficient (Figure 2I and Table S1).²⁶ The intensity and wavelength of emission maxima of the fluorescence spectra also provide information about the physical chemical environment of the Trp residue, both in buffer and when bound to bilayers. To probe the aggregation state of modified peptides in buffer, we also measured the rate of membrane binding using tryptophan fluorescence. Monomeric peptides in buffer bind rapidly to membranes with half-times of just a few seconds (Figure 2F and Table S1). Much slower equilibration, i.e., much longer binding half-times, indicates micelle or aggregate formation in buffer.

We have previously reported that the unmodified peptide, pHD108, is a water-soluble random coil that does not bind to phosphatidylcholine membranes at pH 7 and is not active. ²¹ As pH is decreased below ~6, pHD108 binds to bilayers and forms large pores. Here, pHD108 shows the expected behavior again. In buffer, at pH 7 and at pH 5, the Trp fluorescence of pHD108 has a fluorescence emission maximum ≥ 347 nm (Figure 2D,E), indicating that the Trp residue is mostly water-exposed, and the peptide is not in a self-assembled multimeric structure. This conclusion is supported by the very rapid binding of pHD108 upon lipid addition at pH 5 (Figure 2F and Table S1). Upon binding to POPC at pH 5, the Trp emission maximum is "blueshifted" to a lower wavelength of ~330 nm (Figure 2A,D,E) indicative of a membrane-embedded environment with reduced exposure to water.²⁶ The fluorescence intensity also increases upon binding (Figure 2A-C,G). The mole fraction partition coefficient for pHD108 is 1×10^6 , showing that pHD108 is essentially completely membrane bound at pH 5 (Figure 2H,I, Table S1).

The acylated variants of pHD108 remain in solution in buffer, but most have blue-shifted emission spectra in buffer at both pH 5 and pH 7 (Figure 2D,E) and have binding half-times 50–500 times slower than that of unmodified peptide (Figure 2F), indicating that they are forming micelles or small aggregates in buffer. The only exception is pHD108-C6, the short chain variant, at pH 7, which has a Trp emission maximum and binding half-time consistent with a nonmicellar, monomeric

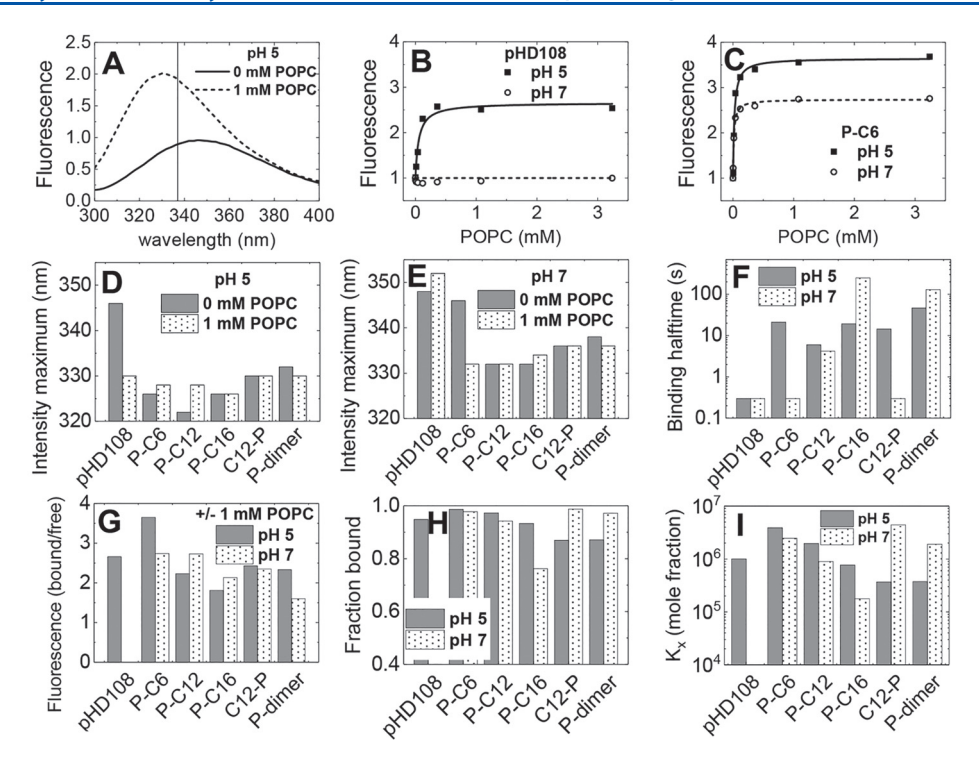


Figure 2. Membrane binding of pHD108 and variants. (A) Example tryptophan fluorescence emission spectra for pHD108 at pH 5 in the absence and presence of POPC vesicles. (B) Example binding curves showing tryptophan fluorescence intensity at 337 nm for pHD108 as POPC vesicle concentration is increased. Increasing intensity (pH 5) indicates membrane binding. Lack of intensity change (pH 7) indicates a lack of binding. (C) Binding curves for pHD108-C6 showing strong binding at pH 5 and pH 7. (D) Wavelength of Trp intensity maximum for pHD108 and its variants with and without POPC vesicles at pH 5. (E) Wavelength of Trp intensity maximum for pHD108 and its variants with and without POPC vesicles at pH 7. (F) Half-time of vesicle binding. Binding was modeled as single exponential process. Rates were extracted from the data and converted to half-times as described in the text. Half-times less than 1 s were not measurable and are upper limits. (G) The increase in Trp fluorescence intensity upon complete binding to POPC. This value is the plateau of time traces such as those shown in panels B and C. (H) The fraction of each peptide bound to 1 mM POPC vesicles at pH 5 and pH 7. (I) Mole fraction partition coefficients for each of the peptides obtained by fitting binding curves as described elsewhere. 26

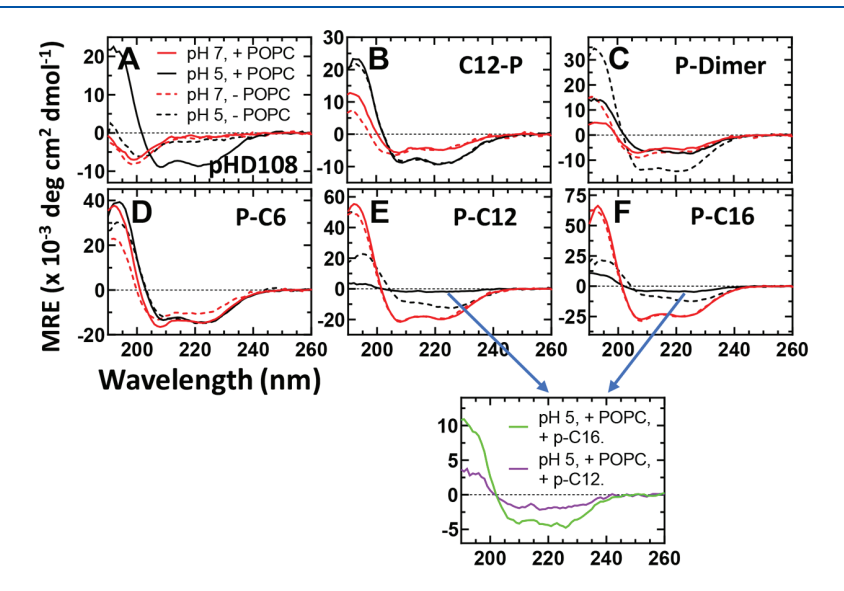


Figure 3. Secondary structure of pHD108 and variants, at pH 5 and pH 7, with and without POPC. (A-F) Solid lines are with POPC and dotted lines are without POPC. Black lines are pH 5 and red lines are pH 7. Nominal peptide concentrations were 30 μ M for all samples. Lipid concentration was 1 mM POPC vesicles. Spectra were obtained in a 1 mm quartz cuvette at room temperature using a JASCO 810 CD spectrometer. Aggregates formed with P-C12 and P-C16 at pH 5 + POPC which reduces the CD signal; therefore, a magnified graph is shown.

structure. Despite the formation of multimers in buffer, all acylated variants bind well to POPC at both pH values (Figure

2H,I). Peptides in micelles equilibrate with the membrane bound state, and the membrane bound state is energetically

preferred. Upon membrane binding, the fluorescence emission intensity increases 1.5–2.5-fold (Figure 2G), enabling the determination of mole fraction partition coefficients (Figure 2I and Table S1), which are high. In the pHD108 dimer, blueshifted Trp emission spectra indicate that there is some oligomerization at both pH values (Figure 2D,E). This conclusion is supported by the long half-times of binding (Figure 2F,G), yet like the acylated variants, the dimer binds well to POPC vesicles even at pH 7 where monomeric pHD108 does not bind (Figure 2H,I).

To examine the secondary structure of the acylated and dimeric variants of pHD108 at pH 5 and pH 7, we used CD spectroscopy with and without the addition of POPC vesicles (Figure 3). For comparison, we show the spectra of unmodified pHD108 in Figure 3A. As previously shown, the helical secondary structure of pHD108 is coupled to pH and membrane binding. The CD spectrum exhibits a single minimum at ~200 nm, indicating a random coil secondary structure at pH 7. This is true both in the presence and absence of lipid vesicles. pHD108 is also unstructured at pH 5 in the absence of vesicles. Only at pH 5 in the presence of vesicles does pHD108 bind and acquire the classical α -helical CD spectrum shown in Figure 3A. In contrast to the unmodified peptide, all acylated and dimeric variants have α -helical secondary structure under all conditions (Figure 3B-F), consistent with the conclusion from fluorescence and binding measurements (Figure 2) that these peptides are not monomeric. Interestingly, the peptide pHD108-C6 in buffer at pH 7 is helical despite lacking other evidence for oligomerization.

Two of the long chain variants, pHD109-C16 and pHD108-C12, although at least partly helical, had ellipticities at pH 5 that were lower than expected, especially in the presence of vesicles. We attribute this loss of intensity to aggregation/fusion of vesicles at pH 5, which we observed, into structures that were too opaque in the far UV spectrum to be observed in CD experiments. Below, we discuss this phenomenon in more detail to explain the lower pore-forming activity of these two peptides under the same conditions.

Pore Formation. We next assessed the pore-forming activity of the acylated pHD peptides at pH 5 and at pH 7. For this, we measured the release of ANTS/DPX, small molecules of \sim 400 Da, as well as the release of TAMRA-biotin dextran (TBD), a macromolecule of 40 000 Da. We describe the potency of each peptide with LIC $_{50}$, the peptide to lipid ratio where the leakage curves cross 50%. Individual leakage curves for ANTS release at the two pH values are shown in Figure 4A. Calculated LIC $_{50}$ values for ANTS leakage are shown in Figure 4B. Leakage curves for TBD release are shown in Figure 5A, and LIC $_{50}$ values for TBD leakage are shown in Figure 5B. LIC $_{50}$ values are listed in Table S1.

The unmodified pHD108 peptide was evolved to be inactive at pH 7, and we have shown that this is because it is not bound to bilayers at this pH. 21 However, this peptide is poised for activity, so as pH is decreased, it begins to bind, fold, and form macromolecule-sized pores that release the contents from vesicles. We show this effect in Figures 4A and 5A, where pHD108 is highly active only at pH 5 and releases both small molecules and macromolecules with similar LIC $_{50}$ values 0.001-0.003, or P:L between \sim 1:1000 and 1:300.

Acylated variants release both small molecules and macromolecules from vesicles at pH 7 with similar LIC_{50} values between 0.0005 and 0.005. These observations provide several important insights. First, they show that either terminus can be

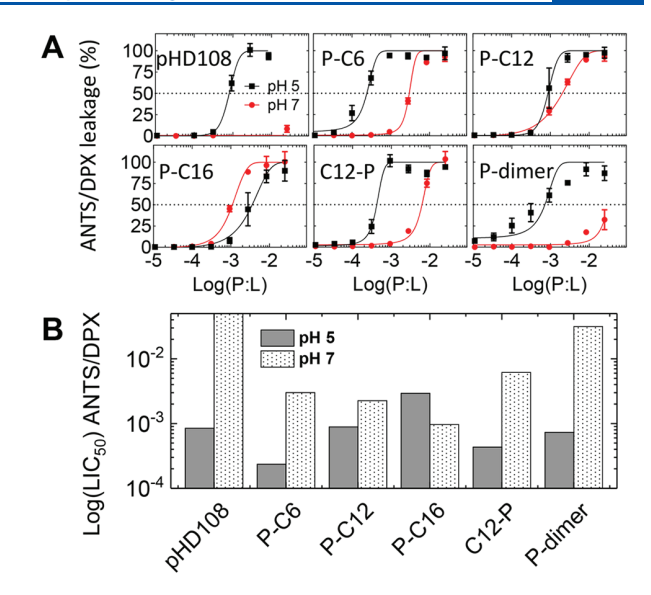


Figure 4. Permeabilization of POPC to the small molecules ANTS and DPX. (A) Permeabilization of POPC vesicles as a function of peptide to lipid ratio (P:L) for pHD108 and its variants at pH 5 and pH 7. Measurements were made 1 h after addition of peptide. (B) The P:L ratio at which a binding curve crosses 50% is the leakage-inducing concentration for 50% or LIC $_{50}$. LIC $_{50}$ values are shown for ANTS/DPX leakage measured 1 h after peptide addition. Lower values indicate more potent activity. Bars that reach the top axis indicate that 50% leakage was not reached at any concentration. Concentration of dimer is expressed relative to the monomeric chains, so leakage curves can be directly compared.

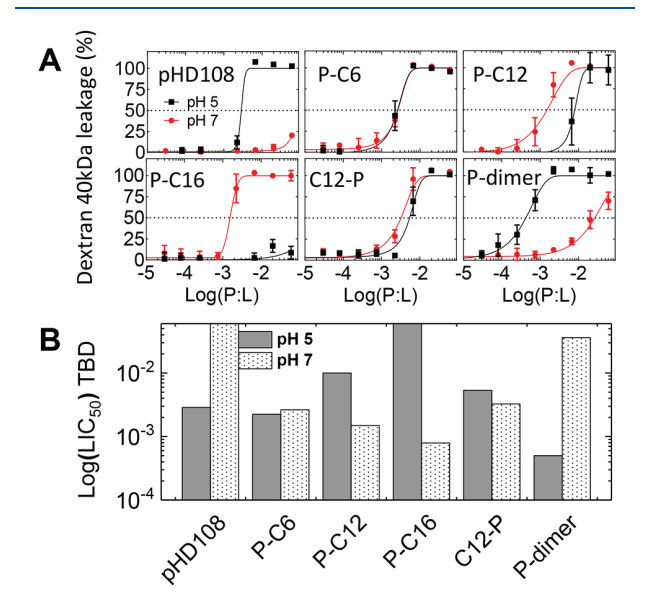


Figure 5. Permeabilization of POPC to the macromolecule TBD (40 kDa). (A) Permeabilization of POPC vesicles to TBD as a function of peptide to lipid ratio (P:L) for pHD108 and its variants at pH 5 and pH 7. Measurements were made 1 h after addition of peptide. (B) Summarized LIC $_{50}$ values. Concentration of dimer is expressed relative to the monomeric chains, so leakage curves can be directly compared.

tethered to the membrane by acyl groups that are as long as 16 carbons and still form the unique structure responsible for macromolecular poration. Second, these observations verify that macromolecular poration can occur without acidic pH; the pHD

peptides can form macromolecule-sized pores at any pH value between 4 and 7, as long as they are membrane bound. At pH 5 the acylated variants are also active for small molecule and macromolecule leakage, but with some additional effects. Some of the variants have similar activity at pH 5 and pH 7 while a few lose activity at pH 5. For example, the pHD108 variant with C12 on the C-terminus loses some macromolecular poration activity relative to its activity at pH 7. The pHD108-C16 variant loses nearly all activity at pH 5.

The dimer of pHD108, with a disulfide cross-link between Cterminal cysteine residues, is highly active, but it retains some of the pH dependence of the parent peptide. The dimer has some activity at pH 7 (Figures 4 and 5) and becomes highly active for small molecule and macromolecule release at pH 5. The pHD108 dimer has the highest macromolecular poration activity recorded in these experiments. At pH 5, the dimer releases both ANTS and TBD with LIC₅₀ of 0.0005, or P:L = 1:2000. This is equivalent to about 50 peptides (25 dimers) per vesicle, which is unprecedented. The slopes of the leakage curves for the dimer are somewhat lower than for the acylated variants. The significance of this is unknown; however, we note that leakage remains hyperbolic (sigmoidal on a semi log plot) under all conditions. Further, the binding kinetics of the dimer are slower than for the acyl variants, and this may affect the leakage mechanism. Comparison of small molecule and macromolecule leakage can provide information about the types of permeabilization events occurring. One of the most interesting characteristics of the pHD peptides is that small molecule and macromolecule leakage occur at similar peptide concentrations. This unusual observation means that most pores in the membrane are large, even at low peptide concentration, and that the peptide does not form small pores preferentially. Small molecule permeabilization without macromolecule permeabilization would indicate nonspecific, surfactant-like membrane disruption. This behavior is very common for membrane-active peptides, but we do not observe it with pHD108 or related family members. At pH 7, the C6-C16 variants all have similar LIC₅₀ values for both small molecule and macromolecule leakage, indicating that the same unique pore structure is being formed by the acylated variants at pH 7 as for the unmodified pHD108 at pH 5. A few differences arise at pH 5 though. For example, macromolecule leakage decreases, but small molecule leakage remains similar for pHD108-C12 and pHD108-C16 at pH 5, indicating that the nature of the macromolecule pore has changed under these specific conditions. This result is consistent with the observation that these two peptides at pH 5 do not have the same secondary structure content as the other peptides.

Lateral Interactions in the Pore. We have previously proposed that the unique macromolecular poration activity of the pHD family of peptides requires that the peptide helices insert into a membrane-spanning conformation. In this configuration, the hydrophobic surfaces of the amphipathic helices would interact with and stabilize the exposed lipids on the pore-water interface on the perimeter of the large pore. It is not known if there are specific lateral interactions between peptides in the pore structure, sometimes called a "barrel-stave" structure, or if the membrane-spanning peptides interact mainly with lipids, called a "toroidal pore" structure. The pHD peptides have three positive charges, two His residues in pHD108, plus the amino terminus, and up to five negative charges, depending on the pH. If there are strong lateral interactions between peptides, they will likely include electrostatic interactions, attractive or repulsive. This is an important hypothesis to test

because, for future optimization, we must know whether it is most fruitful to try to manipulate peptide—lipid interactions or peptide—peptide interactions.

To test the hypothesis that there are lateral electrostatic interactions between peptides in the macromolecule-sized pores, we measured the pHD108-dependent release of TBD in 10 mM acetate buffer with 0 mM and 500 mM KCl and compared it to the leakage curve collected in the presence of 100 mM KCl (Figure 6). Despite the wide range of salt

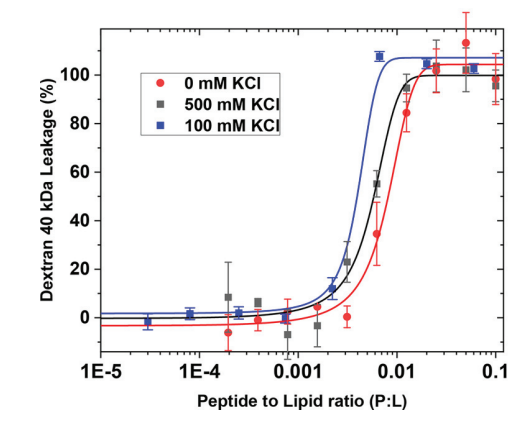


Figure 6. Permeabilization of POPC vesicles to the macromolecule TBD at pH 5 by pHD108. Buffers are 10 mM sodium acetate at pH 5 containing the indicated salt concentration. Solid lines are sigmoidal fits to the data.

concentrations and resultant Debye lengths, which vary from 3 nm down to $\sim\!\!0.4$ nm under these conditions, the leakage curves in Figure 6 are very similar to each other, and the small changes in $\rm LIC_{50}$ do not track linearly with salt. This suggests that the pHD peptides in the macromolecule-sized pores do not have strong lateral, electrostatic peptide—peptide interactions. This conclusion is also supported by the observation that pH does not often affect pore structure or function between pH 4 and 7 (Figures 4 and 5) even though the two histidine residues of pHD108, and many of the acidic residues, will undergo protonation/deprotonation over that range.

DISCUSSION

In this work, we sought to test whether the remarkable macromolecular poration activity of the pHD family peptides can be rationally modulated by acylation or by dimerization, modifications that will increase peptide hydrophobicity and membrane binding potential without changing the amino acid sequence. We also sought to determine which of these modifications are compatible with the macromolecule-sized pores. Finally, we sought evidence for either toroidal or barrel-stave pores by determining if there are dominant lateral electrostatic interactions between peptides in the pore.

Peptide amphiphiles have previously shown increased activity over unmodified peptide in some applications. ^{27,28} In the case of GALA, acylation with C12 and C16 fatty acids increases vesicle permeabilizing activity at pH 5.5 as well as at pH 7.5, ²⁹ where the unmodified GALA peptide is inactive. ⁷ Similarly, conjugation of the SC4 antimicrobial peptide to C12 or C18 fatty acids resulted in up to 30-fold greater bactericidal activity. ²⁸ In both examples, the authors correlated activity with peptide self-assembly, strong helical structure formation, and strong membrane binding.

Dimerization or cross-linking have also been used to increase or modify membrane activity, consistent with the idea that cross-linked pore-forming peptides can represent a preassembled pore state. The antimicrobial peptide magainin, for example, is more active against bacteria and in synthetic vesicles when peptides are cross-linked at the C-terminus by a disulfide linkage. Melittin, from which pHD108 was derived, has also been tested after cross-linking. Cross-linked melittin had variable effects, with decreased activity in PC/cholesterol and PC/phosphatidylglycerol membranes as well as in antimicrobial assays but with increased activity against erythrocytes. Similarly, template-assembled pore-forming peptides have demonstrated greatly increased activities relative to monomeric peptides.

Here, we show that lipidation and dimerization dramatically increase membrane binding and macromolecular poration activity of pHD108 at pH 7. Addition of an acyl group as short as C6 induces membrane binding and high activity at pH7, where unmodified pHD108 is not bound to bilayers and is not active. This supports our previously published conclusion that a low pH is not required for the peptide to form the structure of a macromolecule-sized pore. Instead, pH controls membrane binding of unmodified pHD108, and membrane binding enables macromolecular poration, independent of pH. The observation that acylation can achieve the same result at pH 7 by increased binding provides an important insight into pore properties. The macromolecule-sized pores can form independent of protonation state of the eight ionizable moieties in the peptide. As long as the peptide is membrane bound, it can form large pores.

The pHD108 dimer also retains high activity at pH S where it is even more active than the monomer. At pH S, the LIC $_{50}$ value for macromolecule leakage induced by the dimer is 0.000S, or 1 peptide per 2000 lipids. We know of no other peptide that releases macromolecules from PC bilayers at a concentration this low.

The results presented here also provide insights into pore structure. The acylation results show that C- and N-termini of the pHD peptides can be tethered to bilayers by insertion of a terminal lipid moiety into the bilayer, while still supporting the formation of the unique macromolecule-sized pores. The long chain acyl groups probably insert parallel to the lipid acyl chains. This result suggests that it should be possible to drive increased activity of peptides like these on cells by using other membrane binding motifs attached to the peptide termini to target them to specific cell membranes. Such motifs could include antibodies and nanobodies, receptor ligands, lectins, cationic cell penetrating peptides, or others.

The results give additional clues toward how the pHD family of peptides forms macromolecule-sized pores. Despite the presence of three cationic moieties and five anionic moieties along each α -helix, our data show that macromolecular poration is not strongly dependent on pH (between 5 and 7) or on salt concentration (between 0 and 0.5 M). This is inconsistent with the presence of strong attractive or repulsive electrostatic interactions between the peptides in a barrel-stave-like pore. On the other hand, the data are consistent with a toroidal pore structure in which peptides stabilize the pore perimeter through polar and nonpolar interactions, but mostly with lipids. 23,35

At a minimum, cross-linking has a favorable entropic contribution to pore formation, as it is more favorable to insert one dimer than to insert and assemble two monomers. The high activity of the C-terminal cross-linked parallel pHD108 dimer suggests that the pore structure could contain some parallel

oriented peptides, or mixed parallel and antiparallel peptides. The geometry of the peptides in the pore structure is not known, but parallel helices in the dimer would not need to be in close lateral contact with each other along their length.

Using the insights provided by this work, the pHD peptide family can be further optimized or evolved for specific applications in medicine and cell biology. For example, they could be optimized for cellular specificity by coupling them to a specific receptor ligand or antibody. They could also be developed into peptides that bind to cells at physiological pH, enter into cellular endocytosis pathways, and subsequently drive endosomolysis in response to accumulation in uptake pathways. Peptides with these properties could be used to deliver uptaken macromolecular cargo, including enzymes and antibodies, into the cell cytosol. An alternate target could be the acidic tumor microenvironment, which can trigger the activity of pHtriggered peptides in a similar manner as pHLIP.³⁶ A generation of synthetic molecular evolution can be carried out specifically to identify acylated variants of pHD108 that can induce fine-tuned pH-sensitive membrane permeabilization, activated by the acidic tumor microenvironment. Peptides with such properties may be cytolytic to cancer cells or may synergize with small molecule chemotherapeutics.

CONCLUSION

The pHD peptides are a unique family that enable macromolecular poration of membranes. The data shown here demonstrate that increasing the hydrophobicity of pHD peptides without changing the sequence, by acylation or dimerization, increases membrane binding and subsequent pore-forming activity, even at neutral pH. We therefore confirm previous observations that membrane binding, rather than pH, is a dominant factor in pHD peptide macromolecular poration activity. Both acylation of either termini and dimerization at the C-termini are consistent with a macromolecule-sized pore structure, suggesting that there might be other ways in which the activity of these peptides can be modulated as well. Further information about pore structure comes from the observation that neither pH nor salt concentration significantly affects macromolecular poration. As a result, we propose that pHD108 causes toroidal pores or disordered toroidal pores with parallel or mixed parallel and antiparallel peptides which do not experience strong lateral electrostatic interactions between peptides.

ASSOCIATED CONTENT

Supporting Information

The Supporting Information is available free of charge at https://pubs.acs.org/doi/10.1021/acs.jpcb.0c05363.

Validation of purity of variants, pHD108 vs pHD108-GC comparison, time to reach binding equilibrium, Trp fluorescence emission spectra with 0 and 1 mM POPC, full tryptophan binding curves of conjugates with increasing POPC, and table of variant properties (free energy, rate constant, LIC $_{50}$, etc.) (PDF)

AUTHOR INFORMATION

Corresponding Author

William C. Wimley – Department of Biochemistry and Molecular Biology, Tulane University School of Medicine, New Orleans, Louisiana 70112, United States; orcid.org/0000-0003-

2967-5186; Phone: 504-988-7076; Email: wwimley@tulane.edu

Authors

- Eric Wu Department of Biochemistry and Molecular Biology, Tulane University School of Medicine, New Orleans, Louisiana 70112, United States
- Ramsey M. Jenschke Department of Biochemistry and Molecular Biology, Tulane University School of Medicine, New Orleans, Louisiana 70112, United States
- Kalina Hristova Department of Materials Science and Engineering and Institute for NanoBioTechnology, Johns Hopkins University, Baltimore, Maryland 21218, United States; orcid.org/0000-0003-4274-4406

Complete contact information is available at: https://pubs.acs.org/10.1021/acs.jpcb.0c05363

Notes

The authors declare the following competing financial interest(s): W. Wimley and K. Hristova have filed a US patent application for some of the molecules described herein.

ACKNOWLEDGMENTS

This work was funded by the National Institutes of Health NIH R01 GM111824 (W.C.W.) and the National Science Foundation NSF DMR 1709892 (K.H.) and NSF DMR 1710053 (W.C.W.).

REFERENCES

- (1) Ahmad, A.; Ranjan, S.; Zhang, W.; Zou, J.; Pyykkö, I.; Kinnunen, P. K. J. Novel Endosomolytic Peptides for Enhancing Gene Delivery in Nanoparticles. *Biochim. Biophys. Acta, Biomembr.* **2015**, *1848* (2), 544–553.
- (2) Meyer, M.; Philipp, A.; Oskuee, R.; Schmidt, C.; Wagner, E. Breathing Life into Polycations: Functionalization with PH-Responsive Endosomolytic Peptides and Polyethylene Glycol Enables SiRNA Delivery. J. Am. Chem. Soc. 2008, 130 (11), 3272–3273.
- (3) Kobayashi, S.; Nakase, I.; Kawabata, N.; Yu, H. H.; Pujals, S.; Imanishi, M.; Giralt, E.; Futaki, S. Cytosolic Targeting of Macromolecules Using a PH-Dependent Fusogenic Peptide in Combination with Cationic Liposomes. *Bioconjugate Chem.* 2009, 20 (5), 953–959.
- (4) Plank, C.; Oberhauser, B.; Mechtler, K.; Koch, C.; Wagner, E. The Influence of Endosome-Disruptive Peptides on Gene Transfer Using Synthetic Virus-like Gene Transfer Systems. *J. Biol. Chem.* **1994**, 269 (17), 12918–12924.
- (5) Kakudo, T.; Chaki, S.; Futaki, S.; Nakase, I.; Akaji, K.; Kawakami, T.; Maruyama, K.; Kamiya, H.; Harashima, H. Transferrin-Modified Liposomes Equipped with a PH-Sensitive Fusogenic Peptide: An Artificial Viral-like Delivery System. *Biochemistry* **2004**, *43* (19), 5618–5628.
- (6) Subbarao, N. K.; Parente, R. A.; Szoka, F. C.; Nadasdi, L.; Pongracz, K. PH-Dependent Bilayer Destabilization by an Amphipathic Peptide. *Biochemistry* **1987**, *26* (11), 2964–2972.
- (7) Parente, R. A.; Nir, S.; Szoka, F. C. Mechanism of Leakage of Phospholipid Vesicle Contents Induced by the Peptide GALA. *Biochemistry* **1990**, 29 (37), 8720–8728.
- (8) Wiedman, G.; Fuselier, T.; He, J.; Searson, P. C.; Hristova, K.; Wimley, W. C. Highly Efficient Macromolecule-Sized Poration of Lipid Bilayers by a Synthetically Evolved Peptide. *J. Am. Chem. Soc.* **2014**, *136* (12), 4724–4731.
- (9) Futaki, S.; Masui, Y.; Nakase, I.; Sugiura, Y.; Nakamura, T.; Kogure, K.; Harashima, H. Unique Features of a PH-Sensitive Fusogenic Peptide That Improves the Transfection Efficiency of Cationic Liposomes. *J. Gene Med.* **2005**, *7* (11), 1450–1458.
- (10) Simoes, S.; Slepushkin, V.; Pretzer, E.; Dazin, P.; Gaspar, R.; de Lima, M. C. P.; Duzgunes, N. Transfection of Human Macrophages by

- Lipoplexes via the Combined Use of Transferrin and PH-Sensitive Peptides. J. Leukocyte Biol. 1999, 65 (2), 270-279.
- (11) Zoonens, M.; Reshetnyak, Y. K.; Engelman, D. M. Bilayer Interactions of PHLIP, a Peptide That Can Deliver Drugs and Target Tumors. *Biophys. J.* **2008**, 95 (1), 225–235.
- (12) Wyatt, L. C.; Lewis, J. S.; Andreev, O. A.; Reshetnyak, Y. K.; Engelman, D. M. Applications of PHLIP Technology for Cancer Imaging and Therapy. *Trends Biotechnol.* **2017**, *35*, 653–664.
- (13) Wyatt, L. C.; Moshnikova, A.; Crawford, T.; Engelman, D. M.; Andreev, O. A.; Reshetnyak, Y. K. Peptides of PHLIP Family for Targeted Intracellular and Extracellular Delivery of Cargo Molecules to Tumors. *Proc. Natl. Acad. Sci. U. S. A.* **2018**, *115* (12), E2811–E2818.
- (14) Rinaldi, F.; Hanieh, P. N.; Del Favero, E.; Rondelli, V.; Brocca, P.; Pereira, M. C.; Andreev, O. A.; Reshetnyak, Y. K.; Marianecci, C.; Carafa, M. Decoration of Nanovesicles with PH (Low) Insertion Peptide (PHLIP) for Targeted Delivery. *Nanoscale Res. Lett.* **2018**, *13*. DOI: 10.1186/s11671-018-2807-8
- (15) Andreev, O. A.; Engelman, D. M.; Reshetnyak, Y. K. Targeting Diseased Tissues by PHLIP Insertion at Low Cell Surface PH. *Front. Physiol.* **2014**. DOI: 10.3389/fphys.2014.00097
- (16) Wiedman, G.; Wimley, W. C.; Hristova, K. Testing the Limits of Rational Design by Engineering PH Sensitivity into Membrane-Active Peptides. *Biochim. Biophys. Acta, Biomembr.* **2015**, *1848* (4), 951–957.
- (17) Krauson, A. J.; He, J.; Wimley, W. C. Gain-of-Function Analogues of the Pore-Forming Peptide Melittin Selected by Orthogonal High-Throughput Screening. J. Am. Chem. Soc. 2012, 134 (30), 12732–12741.
- (18) Wimley, W. C. How Does Melittin Permeabilize Membranes? *Biophys. J.* **2018**, *114*, 251–253.
- (19) Wimley, W. C.; Hristova, K. The Mechanism of Membrane Permeabilization by Peptides: Still an Enigma. *Aust. J. Chem.* **2020**, *73*, 96–103.
- (20) Wiedman, G.; Kim, S. Y.; Zapata-Mercado, E.; Wimley, W. C.; Hristova, K. PH-Triggered, Macromolecule-Sized Poration of Lipid Bilayers by Synthetically Evolved Peptides. *J. Am. Chem. Soc.* **2017**, *139* (2), 937–945.
- (21) Kim, S. Y.; Pittman, A. E.; Zapata-Mercado, E.; King, G. M.; Wimley, W. C.; Hristova, K. Mechanism of Action of Peptides That Cause the PH-Triggered Macromolecular Poration of Lipid Bilayers. *J. Am. Chem. Soc.* **2019**, *141* (16), 6706–6718.
- (22) Li, S.; Kim, S. Y.; Pittman, A. E.; King, G. M.; Wimley, W. C.; Hristova, K. Potent Macromolecule-Sized Poration of Lipid Bilayers by the Macrolittins, A Synthetically Evolved Family of Pore-Forming Peptides. J. Am. Chem. Soc. 2018, 140 (20), 6441–6447.
- (23) Wimley, W. C. Describing the Mechanism of Antimicrobial Peptide Action with the Interfacial Activity Model. *ACS Chem. Biol.* **2010**, *5*, 905.
- (24) Sengupta, D.; Leontiadou, H.; Mark, A. E.; Marrink, S. J. Toroidal Pores Formed by Antimicrobial Peptides Show Significant Disorder. *Biochim. Biophys. Acta, Biomembr.* **2008**, 1778 (10), 2308–2317.
- (25) Stewart, J. C. M. Colorimetric Determination of Phospholipids with Ammonium Ferrothiocyanate. *Anal. Biochem.* **1980**, *104* (1), 10–14.
- (26) Ladokhin, A. S.; Jayasinghe, S.; White, S. H. How to Measure and Analyze Tryptophan Fluorescence in Membranes Properly, and Why Bother? *Anal. Biochem.* **2000**, *285* (2), *235*–245.
- (27) Avrahami, D.; Shai, Y. A New Group of Antifungal and Antibacterial Lipopeptides Derived from Non-Membrane Active Peptides Conjugated to Palmitic Acid. *J. Biol. Chem.* **2004**, 279 (13), 12277–12285.
- (28) Lockwood, N. A.; Haseman, J. R.; Tirrell, M. V.; Mayo, K. H. Acylation of SC4 Dodecapeptide Increases Bactericidal Potency against Gram-Positive Bacteria, Including Drug-Resistant Strains. *Biochem. J.* **2004**, 378 (1), 93–103.
- (29) Lin, B. F.; Missirlis, D.; Krogstad, D. V.; Tirrell, M. Structural Effects and Lipid Membrane Interactions of the PH-Responsive GALA Peptide with Fatty Acid Acylation. *Biochemistry* **2012**, *51* (23), 4658–4668.

- (30) Lorenzon, E. N.; Piccoli, J. P.; Santos-Filho, N. A.; Cilli, E. M. Dimerization of Antimicrobial Peptides: A Promising Strategy to Enhance Antimicrobial Peptide Activity. *Protein Pept. Lett.* **2019**, *26* (2), 98–107.
- (31) Mukai, Y.; Matsushita, Y.; Niidome, T.; Hatekeyama, T.; Aoyagi, H. Parallel and Antiparallel Dimers of Magainin 2: Their Interaction with Phospholipid Membrane and Antibacterial Activity. *J. Pept. Sci.* **2002**, *8* (10), 570–577.
- (32) Jamasbi, E.; Batinovic, S.; Sharples, R. A.; Sani, M. A.; Robins-Browne, R. M.; Wade, J. D.; Separovic, F.; Hossain, M. A. Melittin Peptides Exhibit Different Activity on Different Cells and Model Membranes. *Amino Acids* **2014**, *46* (12), 2759–2766.
- (33) Pawlak, M.; Meseth, U.; Vogel, H.; Dhanapal, B.; Mutter, M. Template-assembled Melittin: Structural and Functional Characterization of a Designed, Synthetic Channel-forming Protein. *Protein Sci.* **1994**, 3 (10), 1788–1805.
- (34) Montal, M.; Montal, M. S.; Tomich, J. M. Synporins-Synthetic Proteins That Emulate the Pore Structure of Biological Ionic Channels. *Proc. Natl. Acad. Sci. U. S. A.* **1990**, 87 (18), 6929–6933.
- (35) He, K.; Ludtke, S. J.; Heller, W. T.; Huang, H. W. Mechanism of Alamethicin Insertion into Lipid Bilayers. *Biophys. J.* **1996**, *71* (5), 2669–2679.
- (36) Fendos, J.; Engelman, D. PHLIP and Acidity as a Universal Biomarker for Cancer. *Yale J. Biol. Med.* **2012**, 85 (1), 29–35.